Carbohydrate Polymers 90 (2012) 309–315

Contents lists available at SciVerse ScienceDirect

Carbohydrate Polymers

journal homepage: www.elsevier.com/locate/carbpol

Compared study on the cellulose/$CaCO_3$ composites via microwave-assisted method using different cellulose types

Ming-Guo Ma [a,*], Lian-Hua Fu [a], Run-Cang Sun [a,b], Ning Jia [a]

[a] Institute of Biomass Chemistry and Technology, College of Materials Science and Technology, Beijing Forestry University, Beijing 100083, PR China
[b] State Key Laboratory of Pulp and Paper Engineering, South China University of Technology, Guangzhou 510640, PR China

ARTICLE INFO

Article history:
Received 11 April 2012
Received in revised form 5 May 2012
Accepted 15 May 2012
Available online 22 May 2012

Keywords:
Cellulose
$CaCO_3$
Composites
Microwave
Alkali extraction cellulose
Microcrystalline cellulose

ABSTRACT

The purposes of this study were to explore the influences of different cellulose types on the cellulose/$CaCO_3$ composites, which were synthesized via the microwave-assisted method by using alkali extraction cellulose and microcrystalline cellulose, respectively. Experimental results demonstrated that the types of cellulose played an important role in the microstructure and morphologies of the cellulose/$CaCO_3$ composites. The composites consisted of cellulose and pure phase $CaCO_3$ (calcite). The sample synthesized using microcrystalline cellulose had better crystallinity than that of the sample using alkali extraction cellulose. The cellulose fibers and $CaCO_3$ particles were observed using alkali extraction cellulose. However, using microcrystalline cellulose instead of alkali extraction cellulose, the cellulose with irregular shape and $CaCO_3$ microspheres were obtained. Therefore, choosing appropriate cellulose types is very important for the formation of cellulose/$CaCO_3$ composites. Furthermore, the Raman spectra of the cellulose/$CaCO_3$ composites were also researched.

1. Introduction

As renewable and sustainable resources, cellulose-based materials can be used as engineering materials, forest products, paper, and textiles due to their advantages such as biodegradation, non-petroleum based property, and carbon neutral (Moon, Martini, Nairn, Simonsen, & Youngblood, 2011). Cellulose-based materials provide the possibility for the enhancement of multifunctional properties by using cellulose as matrix compared with the individual components. For example, the cellulose–Ag materials through in situ deposition of silver nanoparticles on the cotton fabrics showed excellent antibacterial activity and laundering durability (Jiang, Liu, & Yao, 2011). Bacterial cellulose-based nanocomposites with tensile strengths of 410 MPa and Young's moduli of 18 GPa were synthesized using LiCl/DMAc as a solvent, which also showed remarkable high toughness characteristic possessing a work-of-fracture as high as 16 MJ m^{-3} (Soykeabkaew, Sian, Gea, Nishino, & Peijs, 2009). $CaCO_3$ is the major inorganic components of shells and limestone. In the previous literature, a poly(vinyl alcohol) hydrogel/$CaCO_3$ composite was prepared by the alternate soaking process as a controlled release support (Ogomi, Serizawa, & Akashi, 2005). Li, Zhu, Cao, and Ma (2009) reported the synthesis of $CaCO_3$ porous hollow microspheres with high drug loading capacity and good drug release properties. The cellulose/$CaCO_3$ composites which enriched the cellulose-based composites family combined the advantages of cellulose and $CaCO_3$.

The cellulose/$CaCO_3$ composites are well known for the biomedical materials and have been receiving more attention due to its biological activities such as protein-adhesive properties, cell compatibility, and hard tissue compatibility (Dalas, Klepetsanis, & Koutsoukos, 2000; Fimbel & Siffert, 1986; Shen, Song, Qian, & Yang, 2010; Subramanian, Maloney, & Paulapuro, 2005; Vilela et al., 2010). Since the first report of cellulose/$CaCO_3$ composites in 1986 (Fimbel & Siffert, 1986), rapid progress has been made in the preparation of cellulose/$CaCO_3$ composites such as the process kinetics of the calcite overgrowth on cellulose substrate (Dalas et al., 2000), the co-precipitation of $CaCO_3$ on pulp (Subramanian et al., 2005), and hierarchical $CaCO_3$ micro- and nanostructures by using cellulose as the templates (Zheng et al., 2007). More recently, cellulose/$CaCO_3$ nanocomposites were investigated by the controlled reaction of $CaCl_2$ with dimethylcarbonate ($(CH_3)_2CO_3$) in alkaline medium in the presence of cellulose fibers (Vilela et al., 2010). Ciobanu, Bobu, and Ciolacu (2010) reported in situ cellulose fibers loading with $CaCO_3$ via three different methods. In previous studies, our group synthesized the cellulose/$CaCO_3$ composites with good biocompatibility via the hydrothermal method by using the cellulose solution, $Ca(NO_3)_2{\cdot}4H_2O$ solution, and $Na_2SiO_3{\cdot}9H_2O$ solution (Jia, Li, Ma, Sun, & Zhu, 2012).

There are a variety of cellulose including wood, plant, tunicate, algae, and bacterial (Hubbe, Rojas, Lucia, & Sain, 2008). Therefore, different cellulose types can be obtained such as microcrystalline cellulose, extraction cellulose from wood and plant, tunicate

* Corresponding author. Tel.: +86 10 62336592; fax: +86 10 62336972.
E-mail address: mg_ma@bjfu.edu.cn (M.-G. Ma).

0144-8617/$ – see front matter © 2012 Elsevier Ltd. All rights reserved.
http://dx.doi.org/10.1016/j.carbpol.2012.05.043

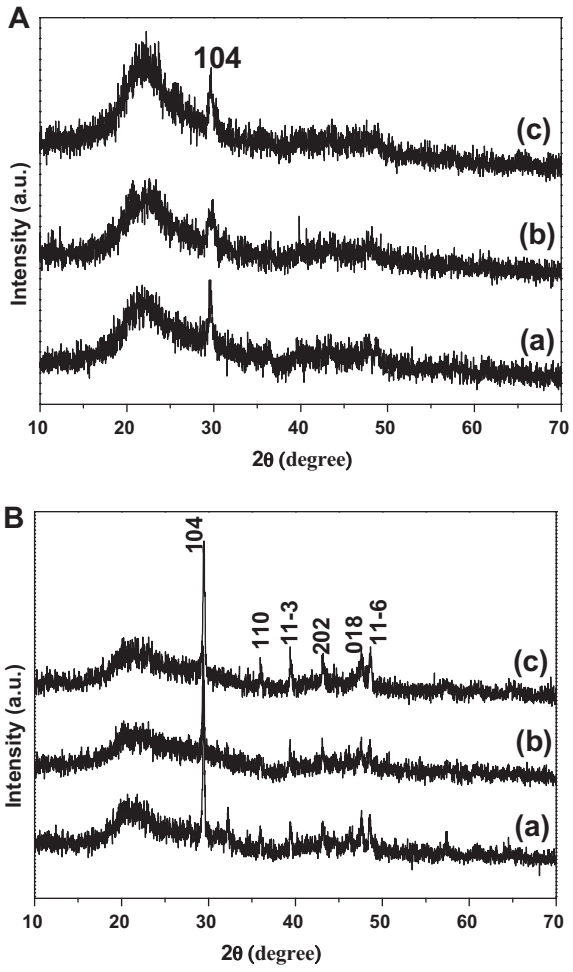

Fig. 1. XRD patterns of the cellulose/$CaCO_3$ composites prepared via microwave heating method by using (A) alkali extraction cellulose and (B) microcrystalline cellulose at 90 °C for different times: (a) 15 min; (b) 30 min; (c) 1 h.

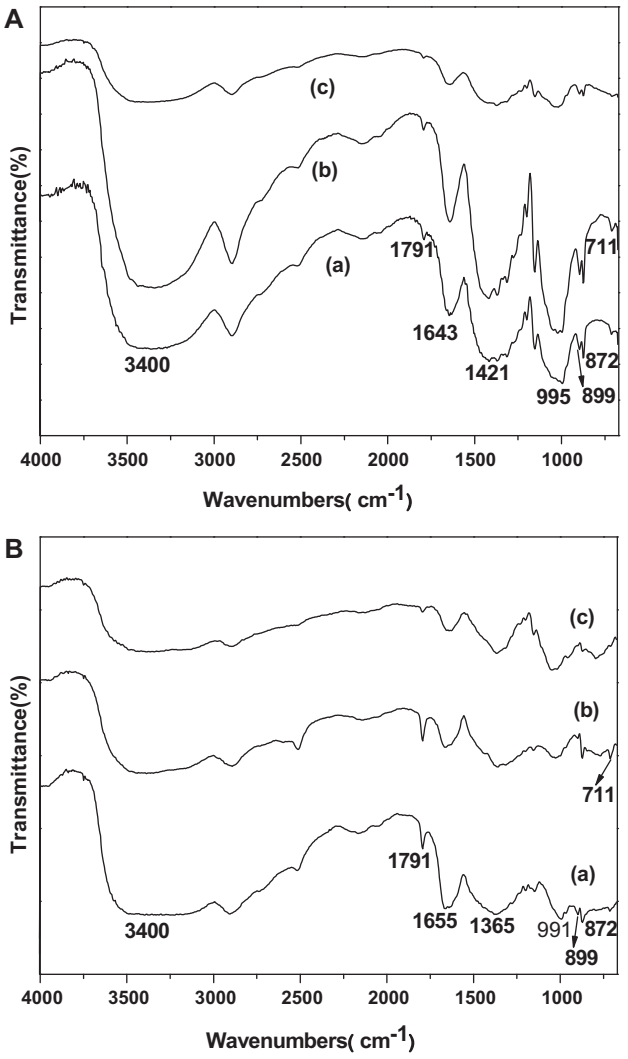

Fig. 2. FTIR spectra of the cellulose/$CaCO_3$ composites prepared via microwave heating method by using (A) alkali extraction cellulose and (B) microcrystalline cellulose at 90 °C for different times: (a) 15 min; (b) 30 min; (c) 1 h.

cellulose, algae cellulose, and bacterial cellulose, which have different characteristic size, aspect ratio, morphology, crystallinity, crystal structure, and properties (Klemm, Heublein, Fink, & Bohn, 2005; Moon et al., 2011). The cellulose types may influence the microstructure and properties of cellulose-based composites.

In this study, we compare study the cellulose/$CaCO_3$ composites via microwave-assisted method by using alkali extraction cellulose and microcrystalline cellulose. The influences of different cellulose types on the phases, microstructure, and morphologies of cellulose/$CaCO_3$ composites were investigated. Microwave-assisted method has been accepted as an efficient technology in materials preparation, thanks to its advantages such as reduced energy consumption, high reaction rate, shorter reaction time, enhanced reaction selectivity, and higher product yield (Tsuji, Hashimoto, Nishizawa, Kubokawa, & Tsuji, 2005).

2. Experimental

2.1. Preparation of cellulose/$CaCO_3$ composites via microwave-assisted method

All chemicals were of analytical grade and used as received without further purification. All experiments were conducted under air atmosphere. Microcrystalline cellulose (molecular weight of 34,843–38,894, degree of polymerization (DP), DP = 215–240) of a commercial reagent was purchased from Sinopharm Group Chemical Reagent Co., Ltd., Shanghai, China. A typical synthesis experiment for the alkali extraction cellulose was carried out as follows: the holocellulose sample was extracted by 10% KOH aqueous solution with a solid to liquid ratio of 1:25 (g mL^{-1}). The mixture was maintained at 25 °C for 16 h. After the pretreatment period, the insoluble residues were separated from the solution by filtration, washed with distilled water until the pH of filtrates was neutral, and then dried at 60 °C. Finally, the alkali extraction cellulose was obtained.

The preparation of cellulose solution followed our previous report (Jia, Li, Ma, Sun, & Zhu, 2010). In a typical experiment, 7.00 g of NaOH and 12.00 g of urea were added into 81 mL of distilled water under vigorous stirring to form NaOH/urea aqueous solution. Then, 3.24 g of cellulose (microcrystalline cellulose or alkali extraction cellulose) was added into the above solution under vigorous stirring. The above solution was cooled to −12 °C for 12 h. The obtained cellulose solution was obtained and applied for the fabrication of cellulose/$CaCO_3$ composites.

For the synthesis of cellulose/$CaCO_3$ composites, 10 mL of $CaCl_2$ solution (0.10 mol/L) and 10 mL of Na_2CO_3 solution (0.10 mol/L) were added into the above cellulose solution (10 mL, 40 g/L) under vigorous stir. The mixture solution was heated to 90 °C and maintained at this temperature for a certain time (15 min or 30 min

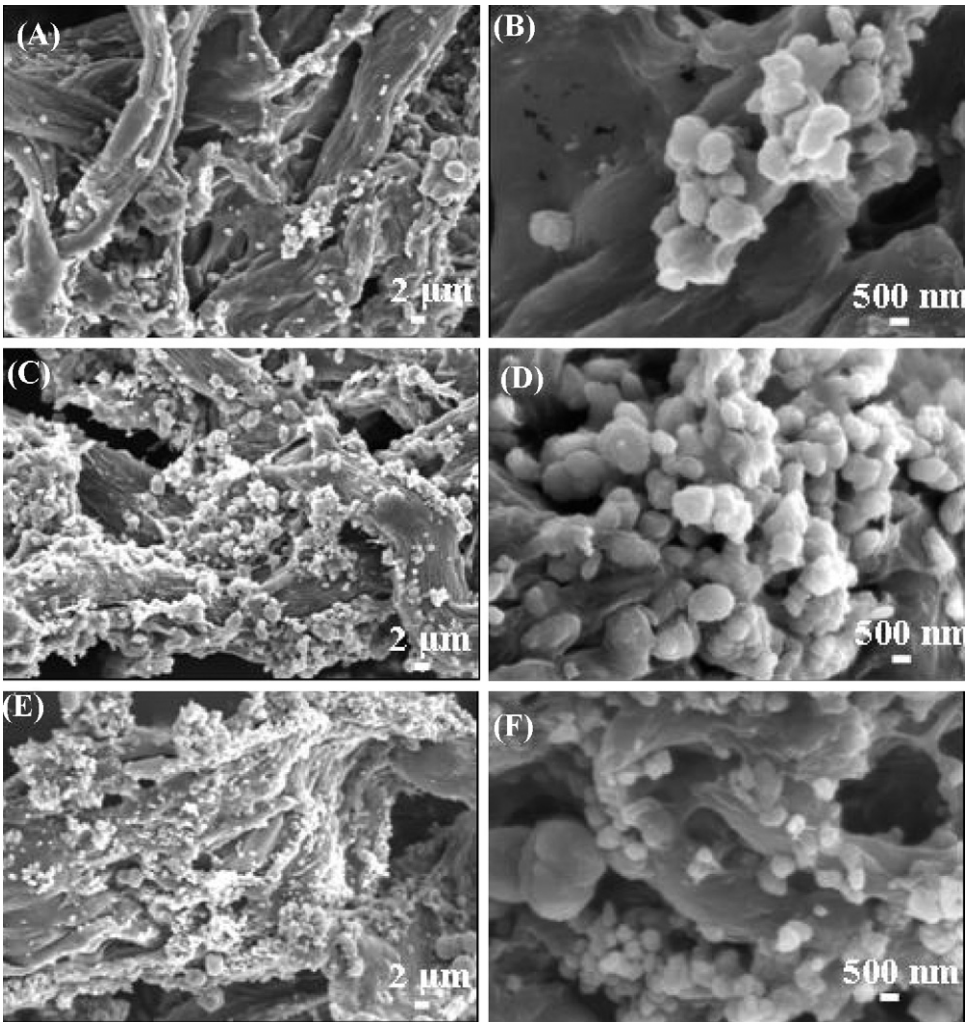

Fig. 3. SEM images of the cellulose/$CaCO_3$ composites prepared by using alkali extraction cellulose at 90 °C for different times: (A and B) 15 min; (C and D) 30 min; (E and F) 1 h.

or 1 h) by microwave heating. The microwave oven used for sample preparation was purchased from Beijing Xiang-Hu Science and Technology Development Reagent Co., Ltd., which was equipped with the magnetic stirring system and a water-cooled condenser outside the microwave cavity. The microwave reactor is an open reaction system. The product was separated from the solution by centrifugation, washed by water and ethanol several times, and dried at 60 °C for further characterization.

2.2. Characterization

X-ray powder diffraction (XRD) was performed in 2θ range from 10° to 70° on a Rigaku D/Max 2200-PC diffractometer with Cu Kα radiation (λ = 0.15418 nm) and graphite monochromator at ambient temperature. Fourier transform infrared (FTIR) spectroscopy was carried out on Thermo Scientific Nicolet iN10 FTIR Microscope (Thermo Nicolet Corporation, Madison, WI, USA), which was equipped with a liquid nitrogen cooled MCT detector. Dried samples were ground and pelletized with BaF_2 and the spectra were recorded in the range of 4000–670 cm^{-1} at 4 cm^{-1} resolution and 128 scans/sample. Scanning electron microscopy (SEM) images were obtained with a Hitachi 3400 N scanning electron microscopy. All samples were Au coated prior to examination by SEM. The energy-dispersive X-ray spectra (EDS) attached to the scanning electron microscopy was used to analyze the composition of sample. Raman spectra of samples were obtained from a LabRam Xplora confocal Raman microscope (Horiba Jobin Yvon) equipped with a confocal microscope (Olympus BX51). Laser light was excited from an emission lamp at λ = 532 nm. The laser power on the sample was approximately 8 mW. The Raman light was detected by an air-cooled, front-illuminated spectroscopic charge-coupled device (CCD) behind a grating (1200 grooves mm^{-1}) spectrometer with a spectral resolution of 2 cm^{-1}. The spectra were recorded from 1800 to 800 cm^{-1}, with a resolution of 2 cm^{-1}.

3. Results and discussion

As we all know, $CaCO_3$ has various types' polymorphs such as calcite, aragonite, and vaterite. Calcite is the thermodynamically stable phase of $CaCO_3$ among of the polymorphs. The phases of the cellulose/$CaCO_3$ composites were characterized with XRD, as shown in Fig. 1. The XRD patterns of the samples prepared by using alkali extraction cellulose via microwave-assisted method at 90 °C displayed the existence of the mixed phases of cellulose (2θ = 21.3° and 22.3°) and calcite with a hexagonal structure (JCPDS 47-1743) (Fig. 1A). Only the peak of (1 0 4) in calcite was clearly observed. One can see that the cellulose/$CaCO_3$ composites were successfully synthesized via microwave-assisted method only within 15 min. Moreover, all the samples had similar XRD patterns, indicating that the heating time had slight influence on the phases and crystallinity

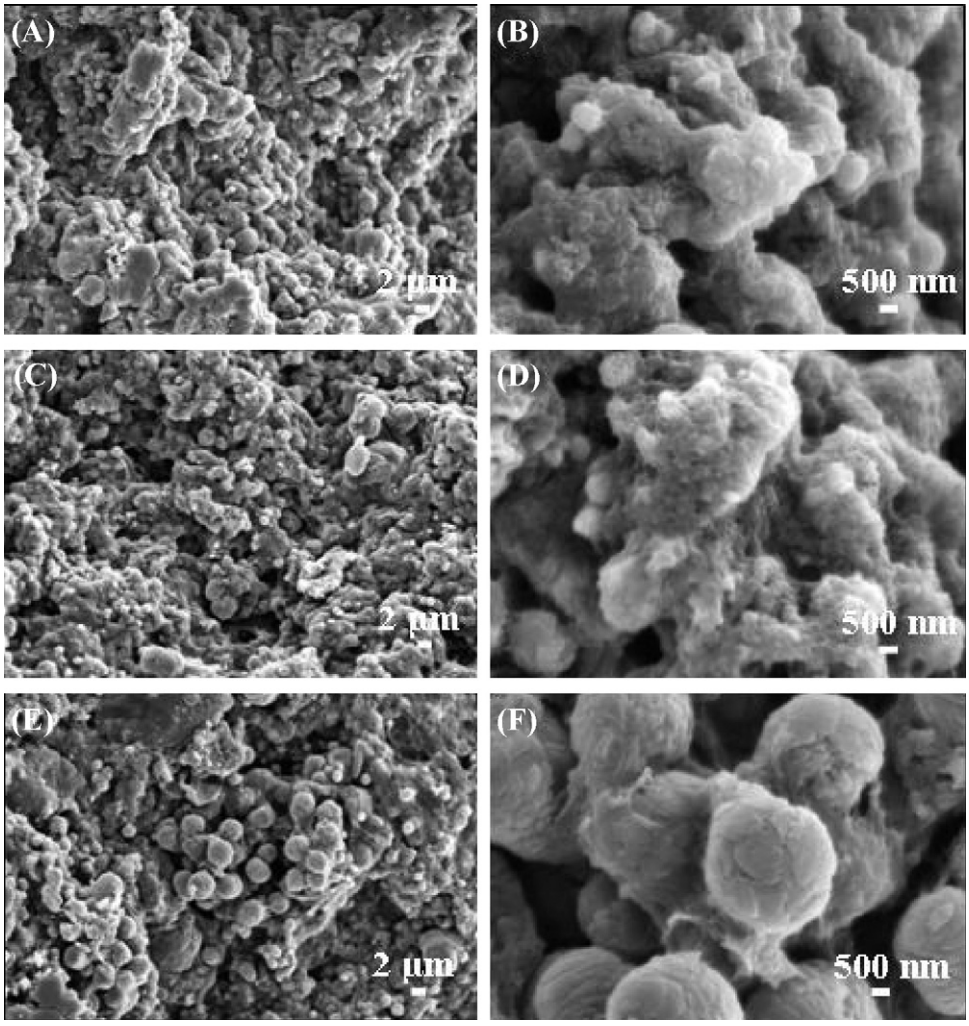

Fig. 4. SEM images of the cellulose/$CaCO_3$ composites prepared by using microcrystalline cellulose at 90 °C for different times: (A and B) 15 min; (C and D) 30 min; (E and F) 1 h.

of the cellulose/$CaCO_3$ composites. Using microcrystalline cellulose instead of alkali extraction cellulose as matrix, the samples also consisted of the mixed phases of cellulose and calcite (Fig. 1B). When the heating time was 15 min, aragonite was observed as a minor phase ($2\theta = 32.2^\circ$), as shown in Fig. 1B(a). When the heating time increased from 15–30 min to 1 h, the aragonite disappeared, pure phase calcite was obtained (Fig. 1B(b) and (c)). The peaks intensity increased with increasing heating time, indicating that the aragonite (metastable phase) was converted to the calcite (thermodynamically stable phase) after longer period of time. In previous study, the similar phenomenon that the aragonite was converted to the calcite with increasing heating time was observed on the synthesis of cellulose/$CaCO_3$ composites via hydrothermal method (Jia et al., 2012). Compared with Fig. 1A, the relative intensity of the peaks was obvious increased, implying that the calcite fabricated by using microcrystalline cellulose had better crystallinity. The alkali extraction cellulose still had minor hemicelluloses and lignin, which restrained the growth of calcite in composites. Of course, the intrinsic and detailed mechanism still needs to be further explored.

FTIR analysis was usually applied to examine the crystal structure of cellulose/$CaCO_3$ composites. The FTIR spectra of the cellulose/$CaCO_3$ composites synthesized by using alkali extraction cellulose showed the typical bands of cellulose at 995 cm^{-1} (the C—O in cellulose) and $CaCO_3$ at around 1421 cm^{-1} (ν_{3-3} CO_3^{2-} and ν_{3-4} CO_3^{2-}) (He, Huang, Liu, Chen, & Xu, 2007; Nelson & Featherstone, 1982), as shown in Fig. 2A. The characteristic stretching mode of calcite were located at around 711 cm^{-1} and 899 cm^{-1} (Donners et al., 2000), while the typical band of aragonite was located at around 872 cm^{-1} (D'Souza et al., 1999; Naka, Keum, Tanaka, & Chujo, 2000). One can see that all of the samples had characteristic bands of calcite and aragonite in Fig. 2A, indicating the existence of calcite and aragonite in cellulose/$CaCO_3$ composites. These results implied that the alkali extraction cellulose not only restrained the growth of calcite in composites, but also restrained the transformation from aragonite to calcite. These results were different from the results of XRD. The XRD patterns of the samples did not display the peaks of aragonite because of the low crystallinity.

The FTIR spectra of the cellulose/$CaCO_3$ composites synthesized by using microcrystalline cellulose were also investigated, as shown in Fig. 2B. When the heating time was 15 min, the characteristic bands of calcite and aragonite were observed in Fig. 2B(a). However, when the heating time was increased to 30 min and 1 h, the typical band of aragonite disappeared and the typical bands of calcite were still observed (Fig. 2B(b) and (c)), demonstrating that the aragonite was converted to calcite with increasing heating time. These results were consistent with the XRD results. From Fig. 2, one can clearly see that both the peaks at 3400 cm^{-1} became broader in the cellulose/$CaCO_3$ composites, compared with that of pure phase cellulose (Li, Jia, Zhu, Ma, & Sun, 2010). In previous study, the similar phenomenon was also observed in other cellulose-based composites (Jia, Li, Ma, Zhu, & Sun, 2011), implying a strong interaction

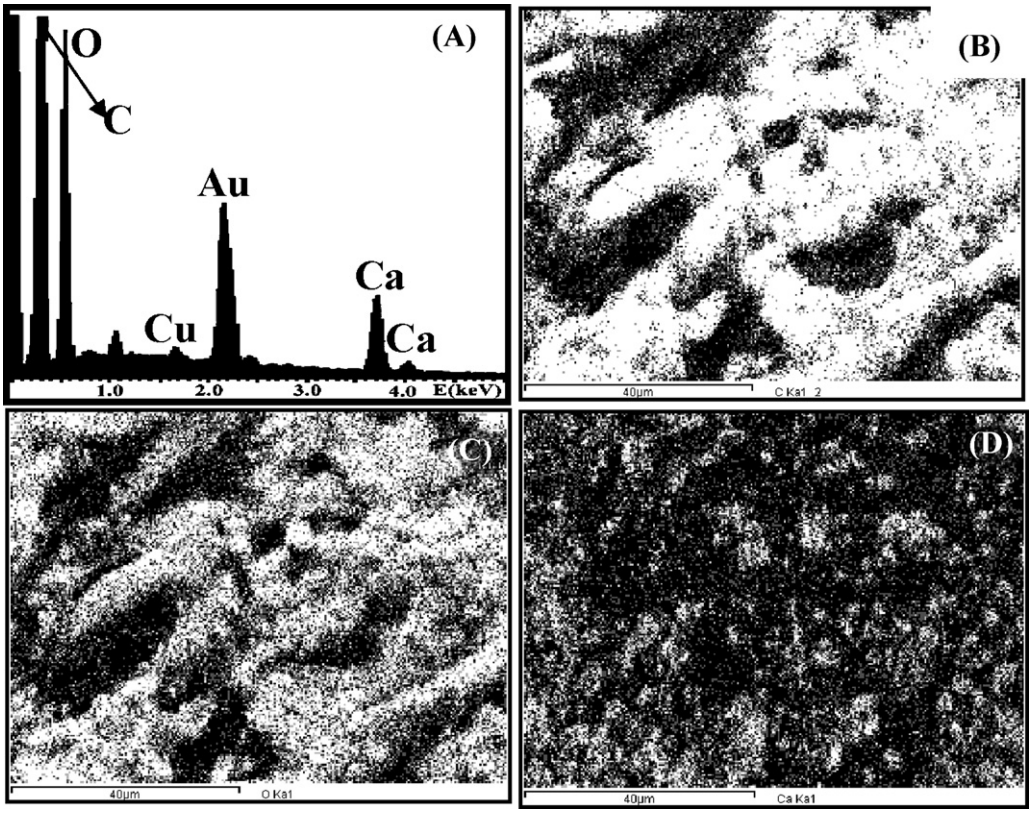

Fig. 5. (A) EDS spectrum and (B–D) the EDS elemental mapping images of the cellulose/$CaCO_3$ composites by using alkali extraction cellulose: (B) C; (C) O; (D) Ca.

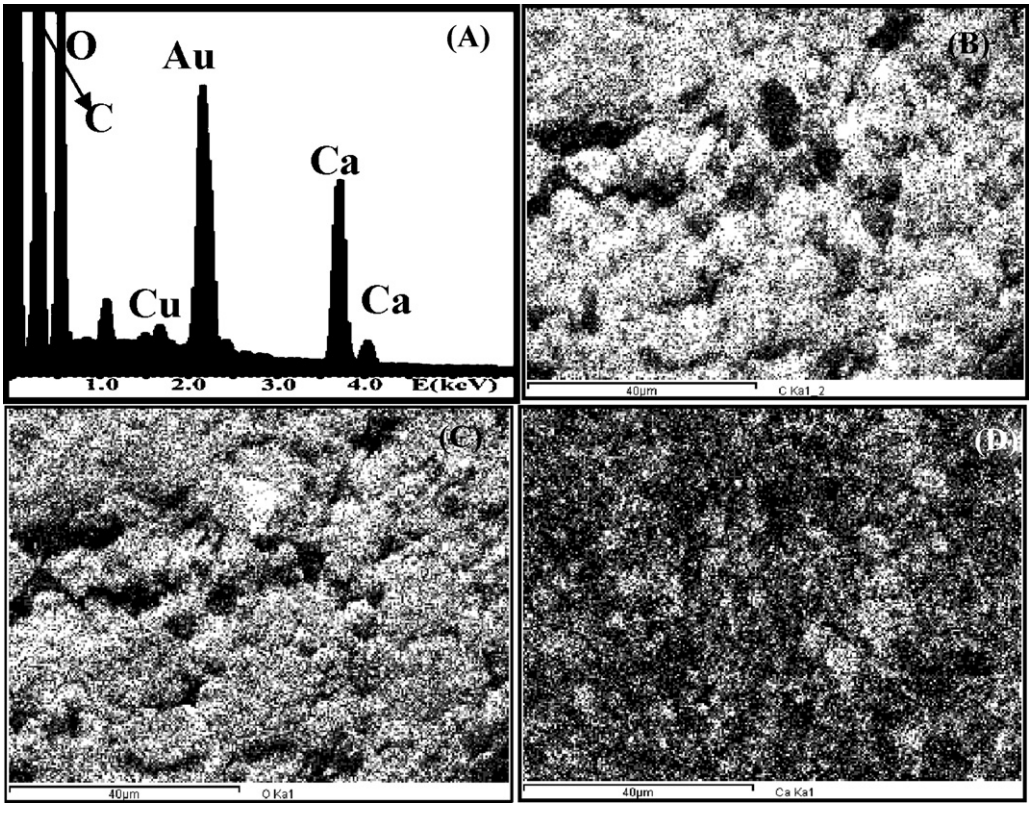

Fig. 6. (A) EDS spectrum and (B–D) the EDS elemental mapping images of the cellulose/$CaCO_3$ composites by using microcrystalline cellulose: (B) C; (C) O; (D) Ca.

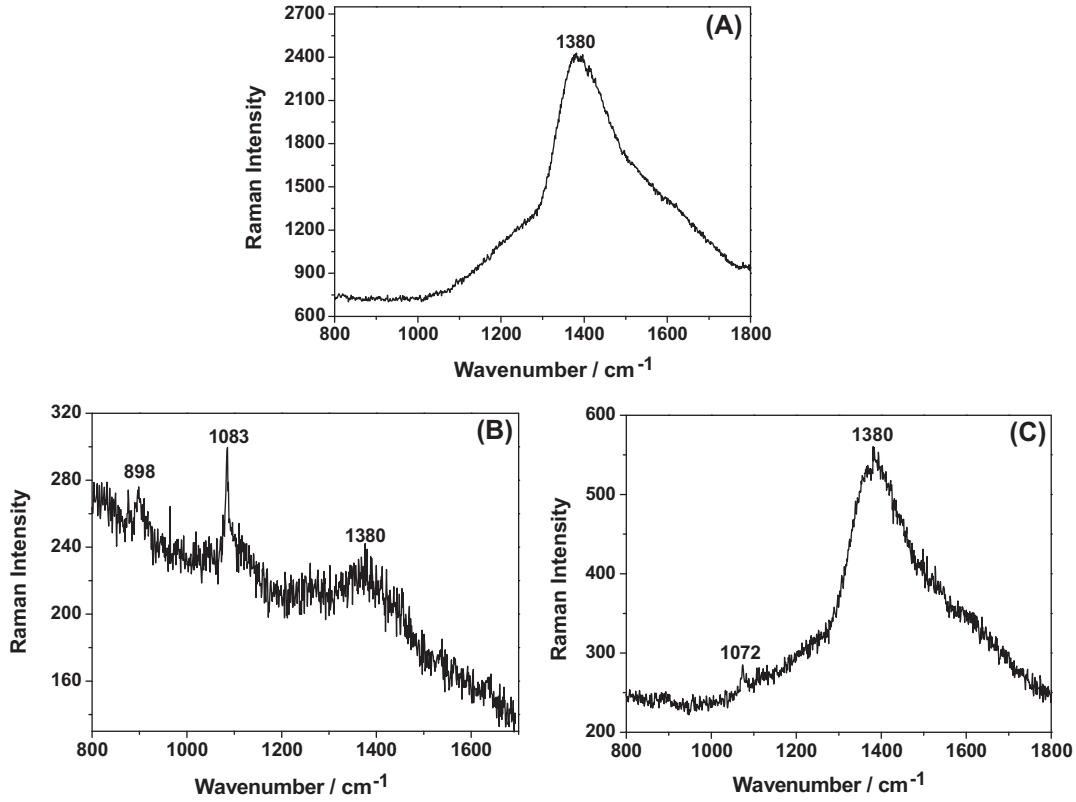

Fig. 7. Raman spectra of: (A) microcrystalline cellulose and (B and C) the cellulose/$CaCO_3$ composites prepared by using (B) alkali extraction cellulose and (C) microcrystalline cellulose at 90 °C for 15 min, respectively.

between the OH group of cellulose and inorganic nanoparticles through hydrogen bonding.

The difference on the morphologies and microstructures of the cellulose/$CaCO_3$ composites synthesized using alkali extraction cellulose and microcrystalline cellulose were also investigated with SEM. The SEM images of the samples synthesized by using alkali extraction cellulose were shown in Fig. 3. One can see that the cellulose has fiber-like shape and the $CaCO_3$ particles grow on cellulose substrate. Magnified micrographs of the composites were shown in Fig. 3B, D, and F. When the heating time was 15 min, the size of the $CaCO_3$ particles was around 1 μm (Fig. 3B). The size of $CaCO_3$ particles decreased to around 500 nm and number of $CaCO_3$ particles increased with the increasing heating time (Fig. 3F). For comparison, using microcrystalline cellulose instead of alkali extraction cellulose, the SEM images of the samples were shown in Fig. 4. From which one can see the cellulose with irregular morphology and $CaCO_3$ with microsphere-like shape. $CaCO_3$ microspheres were disappeared on the surface of irregular cellulose. Magnified micrographs of the $CaCO_3$ microspheres were shown in Fig. 4B, D, and F. When the heating time was 15 min, the size of $CaCO_3$ spheres was around 700 nm (Fig. 4B). As the heating time increased to 1 h, the size of $CaCO_3$ microspheres was increased to around 3.5 μm (Fig. 4F). These results demonstrated that the size of $CaCO_3$ spheres was dramatically increased with increasing heating time, which was different from the results in Fig. 3. The size of $CaCO_3$ spheres was obviously increased and the cellulose had a completely different morphology, which was due to the difference of the cellulose types, indicating that the cellulose types not only had an effect on the phase, but also played an important role in the shape of cellulose/$CaCO_3$ composites. Therefore, choosing appropriate cellulose is very important for the formation of cellulose/$CaCO_3$ composites. The synthesis of $CaCO_3$ spheres included the nucleation, growth, ripening, etc. When plenty of nucleation happened, the growth was restrained and relatively small particles were obtained. However, when the few of nucleation happened, the particles growth with increasing heating time and relatively big particles were obtained. In view of the above results, one can conclude that the nucleation was the key step for the synthesis of $CaCO_3$ particles by using alkali extraction cellulose. On the contrary, the growth was the key step for the synthesis of $CaCO_3$ microspheres by using microcrystalline cellulose as substrate.

The EDS spectrum and the EDS elemental mapping were applied to investigate the dispersion of $CaCO_3$ on the cellulose matrix. The EDS spectrum (Fig. 5A) displayed that the sample synthesized by using alkali extraction cellulose consisted of C, O, and Ca, the right compositions of cellulose/$CaCO_3$ composites. The Cu peak is originated from the copper sample holder. The Au peak came from the preparation procedure of samples prior to examination by SEM. Fig. 5B–D showed the EDS elemental mapping images of C, O, and Ca, respectively, and further confirmed the composition of cellulose/$CaCO_3$ composites and the even distribution of $CaCO_3$ particles.

The EDS spectrum (Fig. 6A) and the EDS elemental mapping images (Fig. 6B–D) of the cellulose/$CaCO_3$ composites synthesized by using microcrystalline cellulose showed similar results. The peak intensity of Ca in EDS spectrum increased compared with Fig. 5A, indicating the high concentration of $CaCO_3$ in composites. These results were consistent with the previous XRD results. Moreover, from the elemental mapping image of Ca in Fig. 6D, the $CaCO_3$ had more wide distribution than that of Fig. 5D, which was consistent with the previous SEM results. From the SEM images of Figs. 3 and 4, the $CaCO_3$ particles were dispersed on the alkali extraction cellulose matrix, while the $CaCO_3$ microspheres were dispersed on the microcrystalline cellulose matrix. Numbers of $CaCO_3$ microspheres were more than that of particles on the surface of cellulose.

Raman spectra were known to be sensitive for detecting polymorphic changes of the cellulose-based composites (Atalla, 1976), as shown in Fig. 7B and C. For comparison, the Raman spectrum of microcrystalline cellulose is also shown in Fig. 7A, from which one can see that a very strong peak located at 1380 cm^{-1} was observed, assigning to the HCC, HCO, COH, and CH_2 deformation (Adebajo, Frost, Kloprogge, & Kokot, 2006; Wiley & Atalla, 1987). However, the relative peak intensity of the cellulose/$CaCO_3$ composites using alkali extraction cellulose significantly decreased and became narrow (Fig. 7B), compared with Fig. 7A. Moreover, the sharp peak at 1083 cm^{-1} appeared, attributing to the combination vibration modes from C—O—C glycosidic linkage deformation, ring breathing symmetric stretching (Kong & Eichhorn, 2005; Kong, Wilding, Ibbett, & Eichhorn, 2008). The weak peak at 898 cm^{-1} is assigned to the methine group at C1 (Blackwell, Vasko, & Koenig, 1970; Cael, Gardner, Koenig, & Blackwell, 1975). Using microcrystalline cellulose instead of alkali extraction cellulose, the peak intensity of the cellulose/$CaCO_3$ composites at 1380 cm^{-1} dramatically decreased (Fig. 7C), compared with Fig. 7A. A weak peak at 1072 cm^{-1} was also observed, which was assigned to the combination vibration modes from C—O—C glycosidic linkage deformation, ring breathing symmetric stretching (Kong & Eichhorn, 2005; Kong et al., 2008).

4. Conclusions

In summary, we reported the synthesis of the cellulose/$CaCO_3$ composites via microwave-assisted method by using alkali extraction cellulose and microcrystalline cellulose, respectively. XRD and FTIR results revealed that the samples synthesized by using microcrystalline cellulose had better crystallinity, and composites of cellulose and $CaCO_3$ (calcite) were obtained. However, when alkali extraction cellulose was used, the mixed phases of cellulose, calcite, and aragonite with poor crystallinity were observed. Cellulose fibers and $CaCO_3$ particles were observed by using alkali extraction cellulose. The cellulose with irregular shape and $CaCO_3$ microspheres were obtained by using microcrystalline cellulose. Experimental results demonstrated that the cellulose types played an important role in the shapes and microstructures of cellulose/$CaCO_3$ composites.

Acknowledgments

Financial supported by the Program for New Century Excellent Talents in University (NCET-11-0586), National Natural Science Foundation of China (31070511), and Major State Basic Research Development Program of China (973 Program) (No. 2010CB732204) is gratefully acknowledged.

References

Adebajo, M. O., Frost, R. L., Kloprogge, J. T., & Kokot, S. (2006). Raman spectroscopic investigation of acetylation of raw cotton. *Spectrochimica Acta Part A: Molecular and Biomolecular Spectroscopy*, *64*, 448–453.

Atalla, R. H. (1976). Raman spectral studies of polymorphy in cellulose. I: Celluloses I and II. *Applied Polymer Symposium*, *28*, 659–669.

Blackwell, J., Vasko, P. D., & Koenig, J. L. (1970). Infrared and Raman spectra of the cellulose from the cell wall of *Valonia ventricosa*. *Journal of Applied Physics*, *41*, 4375–4379.

Cael, J. J., Gardner, K. H., Koenig, J. L., & Blackwell, J. (1975). Infrared and Raman spectroscopy of carbohydrates. Paper V: Normal co-ordinate analysis of cellulose. *Journal of Chemical Physics*, *62*, 1145–1153.

Ciobanu, M., Bobu, E., & Ciolacu, F. (2010). In situ cellulose fibres loading with calcium carbonate precipitated by different methods. *Cellulose Chemistry and Technology*, *44*, 379–387.

Dalas, E., Klepetsanis, P. G., & Koutsoukos, P. G. (2000). Calcium carbonate deposition on cellulose. *Journal of Colloid Interface Science*, *224*, 56–62.

Donners, J. J. J. M., Heywood, B. R., Meijier, E. W., Nolte, R. J. M., Roman, C., Schenning, A. P. H. J., et al. (2000). Amorphous calcium carbonate stabilized by poly(propylene imine) dendrimers. *Chemical Communications*, 1937–1938.

D'Souza, S. M., Alexander, C., Carr, S. W., Waller, A. M., Whitcombe, M. J., & Vulfson, E. N. (1999). Directed nucleation of calcite at a crystal-imprinted polymer surface. *Nature*, *398*, 312–316.

Fimbel, P., & Siffert, B. (1986). Interaction of calcium carbonate (calcite) with cellulose fibres in aqueous medium. *Colloids and Surfaces*, *20*, 1–16.

He, Q., Huang, Z., Liu, Y., Chen, W., & Xu, T. (2007). Template-directed one-step synthesis of flowerlike porous carbonated hydroxyapatite spheres. *Materials Letters*, *61*, 141–143.

Hubbe, M. A., Rojas, O. J., Lucia, L. A., & Sain, M. (2008). Cellulosic composites: A review. *BioResources*, *3*, 929–980.

Jia, N., Li, S. M., Ma, M. G., Sun, R. C., & Zhu, J. F. (2010). Hydrothermal synthesis and characterization of cellulose-carbonated hydroxyapatite composites in NaOH–urea aqueous solution. *Science of Advanced Materials*, *2*, 210–214.

Jia, N., Li, S. M., Ma, M. G., Sun, R. C., & Zhu, J. F. (2012). Hydrothermal fabrication, characterization, and biological activity of cellulose/$CaCO_3$ biocomposites. *Carbohydrate Polymer*, *88*, 179–184.

Jia, N., Li, S. M., Ma, M. G., Zhu, J. F., & Sun, R. C. (2011). Synthesis and characterization of cellulose–silica composite fiber in ethanol/water mixed solvents. *BioResources*, *62*, 1186–1195.

Jiang, T., Liu, L., & Yao, J. M. (2011). In situ deposition of silver nanoparticles on the cotton fabrics. *Fibers and Polymers*, *12*, 620–625.

Klemm, D., Heublein, B., Fink, H. P., & Bohn, A. (2005). Cellulose: Fascinating biopolymer and sustainable raw material. *Angewandte Chemie International Edition*, *44*, 3358–3393.

Kong, K., & Eichhorn, S. J. (2005). The influence of hydrogen bonding on the deformation micromechanics of cellulose fibers. *Journal of Macromolecular Science, Part B: Physics B*, *44*, 1123–1136.

Kong, K., Wilding, M. A., Ibbett, R. N., & Eichhorn, S. (2008). Molecular and crystal deformation of cellulose: Uniform strain or uniform stress? *Faraday Discussions*, *139*, 283–298.

Li, L., Zhu, Y. J., Cao, S. W., & Ma, M. Y. (2009). Preparation and drug release properties of nanostructured $CaCO_3$ porous hollow microspheres. *Journal of Inorganic Materials*, *24*, 166–170.

Li, S. M., Jia, N., Zhu, J. F., Ma, M. G., & Sun, R. C. (2010). Synthesis of cellulose–calcium silicate nanocomposites in ethanol/water mixed solvents and their characterization. *Carbohydrate Polymers*, *80*, 270–275.

Moon, R. J., Martini, A., Nairn, J., Simonsen, J., & Youngblood, J. (2011). Cellulose nanomaterials review: Structure, properties and composites. *Chemical Society Reviews*, *40*, 3941–3994.

Naka, K., Keum, D. K., Tanaka, Y., & Chujo, Y. (2000). Control of crystal polymorphs by a 'latent inductor': Crystallization of calcium carbonate in conjunction with in situ radical polymerization of sodium acrylate in aqueous solution. *Chemical Communications*, 1537–1538.

Nelson, D. G. A., & Featherstone, J. D. B. (1982). Preparation, analysis, and characterization of carbonated apatites. *Calcified Tissue International*, *34*, 69–81.

Ogomi, D., Serizawa, T., & Akashi, M. (2005). Controlled release based on the dissolution of a calcium carbonate layer deposited on hydrogels. *Journal of Controlled Release*, *103*, 315–323.

Shen, J., Song, Z. Q., Qian, X. R., & Yang, F. (2010). Carboxymethyl cellulose/alum modified precipitated calcium carbonate fillers: Preparation and their use in papermaking. *Carbohydrate Polymers*, *81*, 545–553.

Soykeabkaew, N., Sian, C., Gea, S., Nishino, T., & Peijs, T. (2009). All-cellulose nanocomposites by surface selective dissolution of bacterial cellulose. *Cellulose*, *16*, 435–444.

Subramanian, R., Maloney, T., & Paulapuro, H. (2005). Calcium carbonate composite fillers. *Tappi Journal*, *4*, 23–27.

Tsuji, M., Hashimoto, M., Nishizawa, Y., Kubokawa, M., & Tsuji, T. (2005). Microwave-assisted synthesis of metallic nanostructures in solution. *Chemistry: A European Journal*, *11*, 440–452.

Vilela, C., Freire, C. S. R., Marques, P. A. A. P., Trindade, T., Neto, C. P., & Fardim, P. (2010). Synthesis and characterization of new $CaCO_3$/cellulose composites prepared by controlled hydrolysis of dimethylcarbonate. *Carbohydrate Polymers*, *79*, 1150–1156.

Wiley, J. H., & Atalla, R. H. (1987). Bands assignments in the Raman spectra of celluloses. *Carbohydrate Research*, *160*, 113–129.

Zheng, Z., Huang, B. J., Ma, H. Q., Zhang, X. P., Liu, Z., Wong, K. W., et al. (2007). Biomimetic growth of biomorphic $CaCO_3$ with hierarchically ordered cellulosic structures. *Crystal Growth and Design*, *7*, 1912–1917.